International Conference on the Initial Stages in High-Energy Nuclear Collisions

Centrality dependence of charged particle production in proton-lead collisions measured by ATLAS (based on ATLAS-CONF-2013-096)

Evgeny Shulga

for the ATLAS Collaboration

National Research Nuclear University "MEPhI"

Content

- **Existing results**

- **ATLAS detector**
- **2012 pilot p+Pb run @ LHC**

- **Event selection**
  - **Summary**
  - **Edge-gap selection**

- **Centrality**
  - **Glauber and Glauber-Gribov model**
  - **FCal ΣE_T distribution**

- **Charged particle pseudorapidity density**
  - **Pixel tracks and pixel tracklet methods**
  - **Corrections**
  - **Systematics**
  - **Results**
  - **Model dependence**

- **Conclusion**

Introduction

p/d+A collisions at the LHC and RHIC provide an opportunity to study the physics of the initial-state of ultra-relativistic A+A collisions without of thermalization and collective evolution

- p/d+A measurements can shed insight on the:
  - impact of an extended nuclear target
  - the dynamics of soft and hard scattering processes
  - subsequent particle production

- $dN_{ch}/d\eta$ vs η is the most basic experimental probe which as a function of centrality can provide understanding of p+A interactions

RHIC energies

- Centrality dependence of the charged particle production @ RHIC
- Scaling with N_{part} have been previously observed

PHOBOS

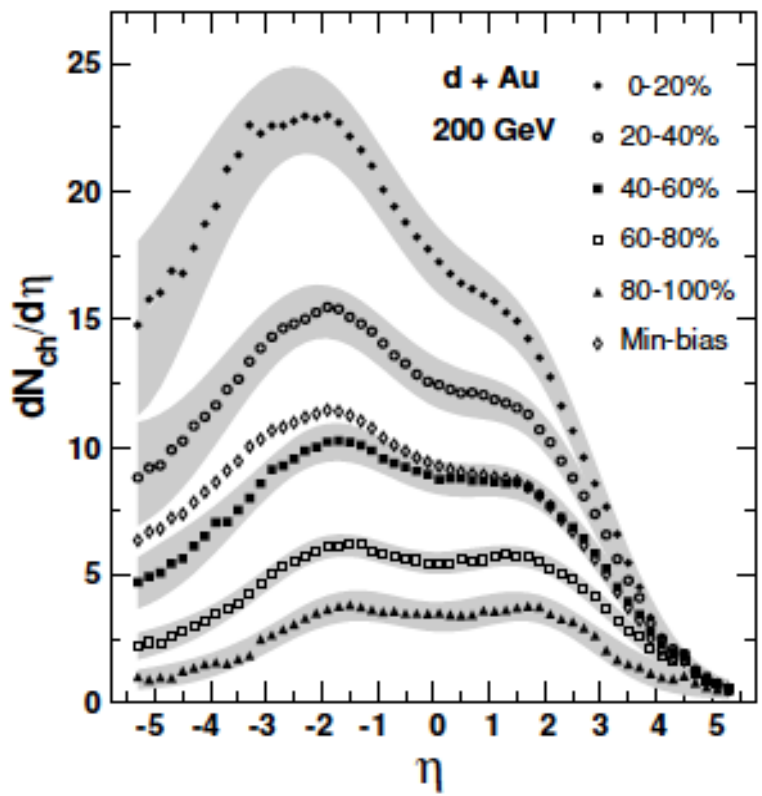

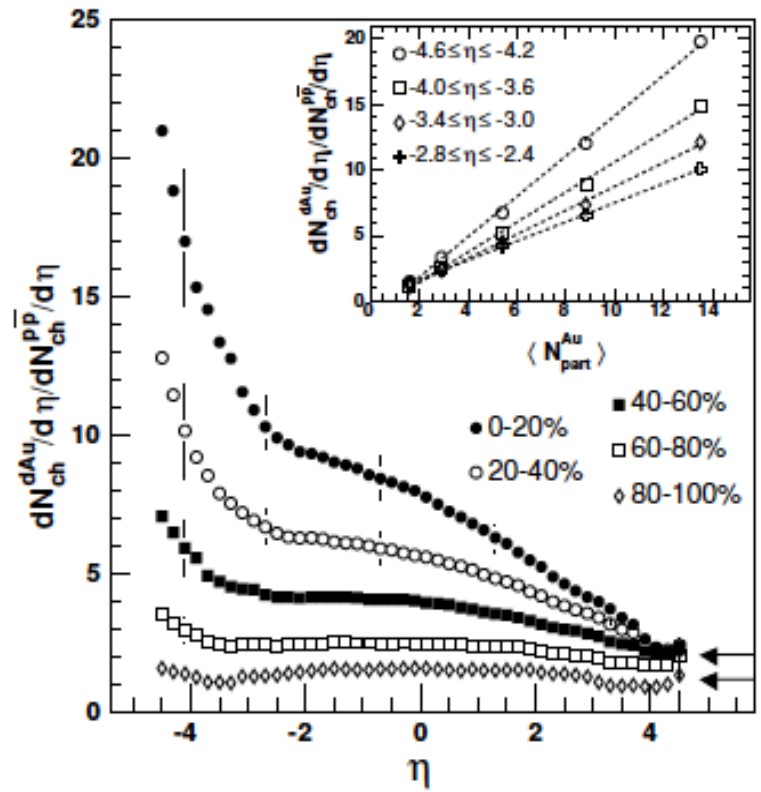

PHYSICAL REVIEW C 72, 031901(R) (2005)

Existing results

- ALICE measured MB (non-singly diffractive) $dN_{ch}/d\eta$ vs η.
- The centrality dependence is important and it is not yet measured.

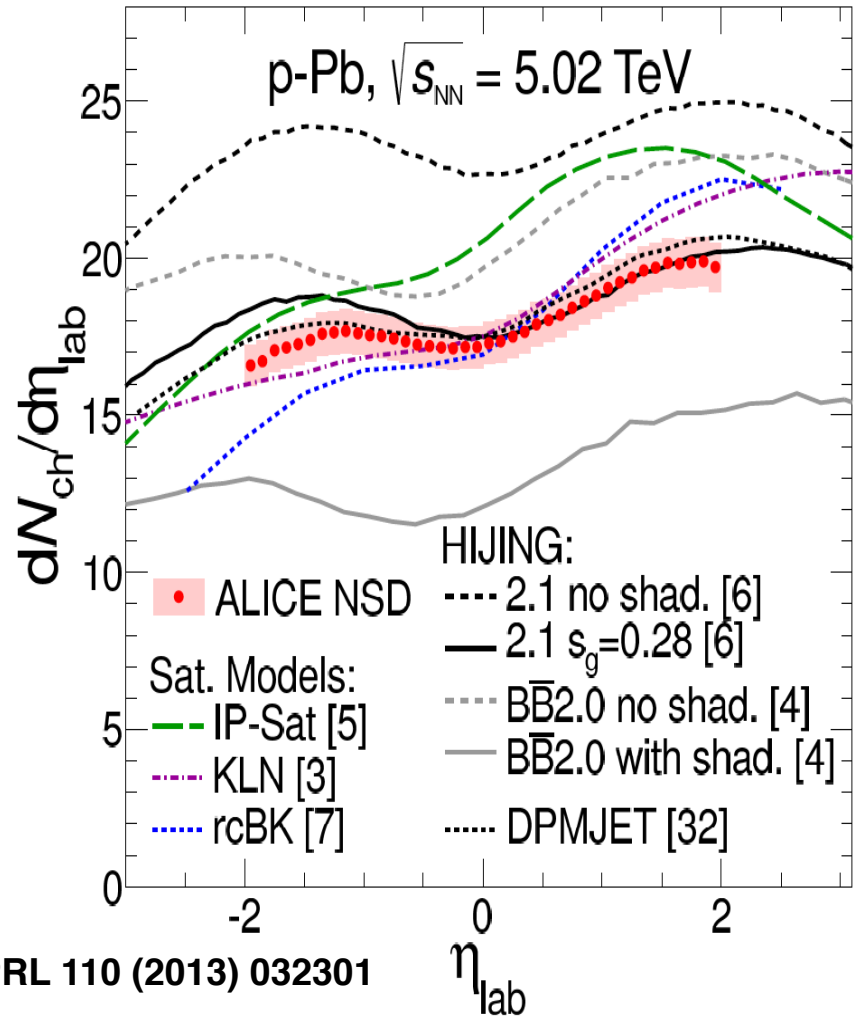

PRL 110 (2013) 032301

p+Pb @ LHC and ATLAS

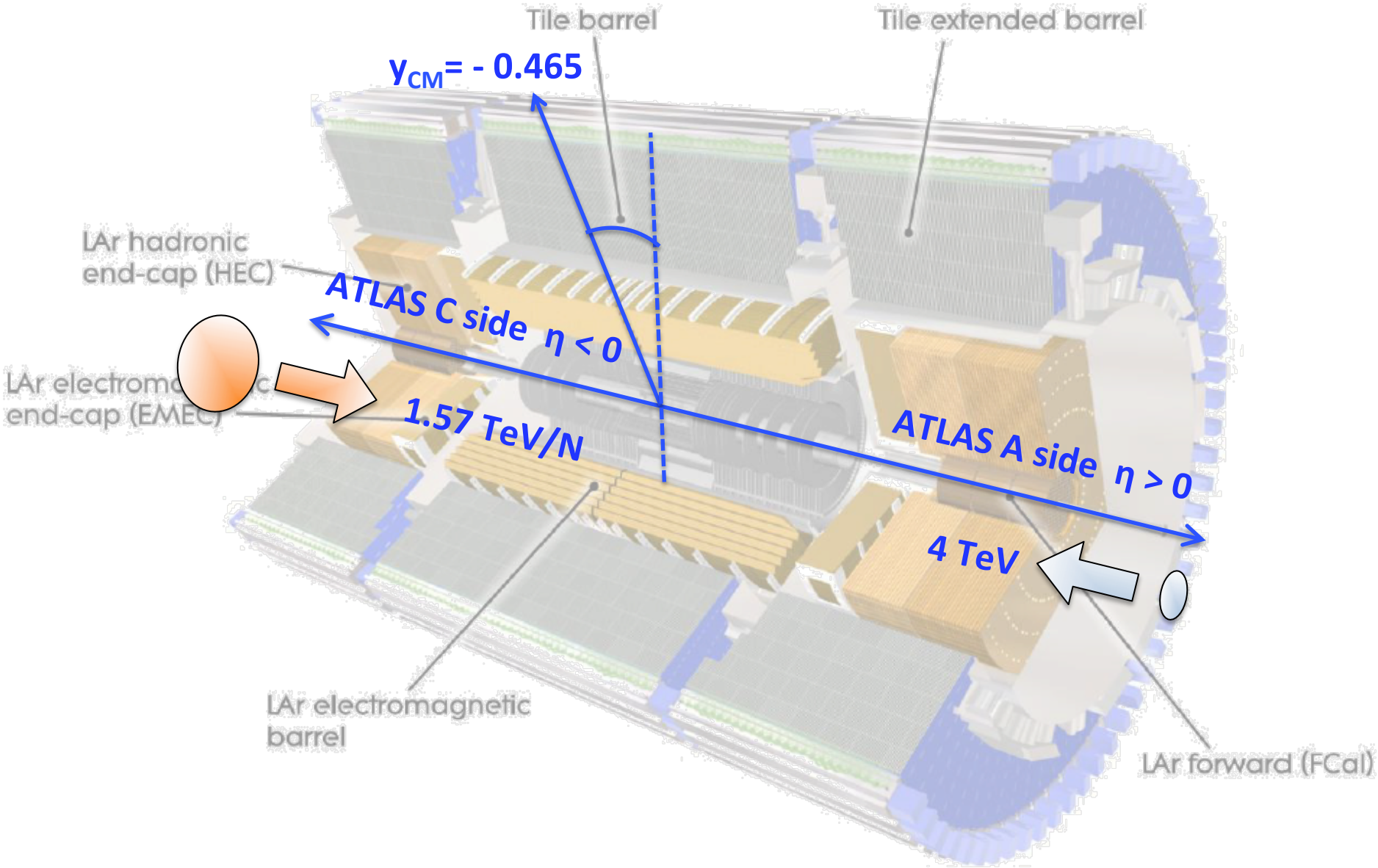

p+Pb @ LHC and ATLAS

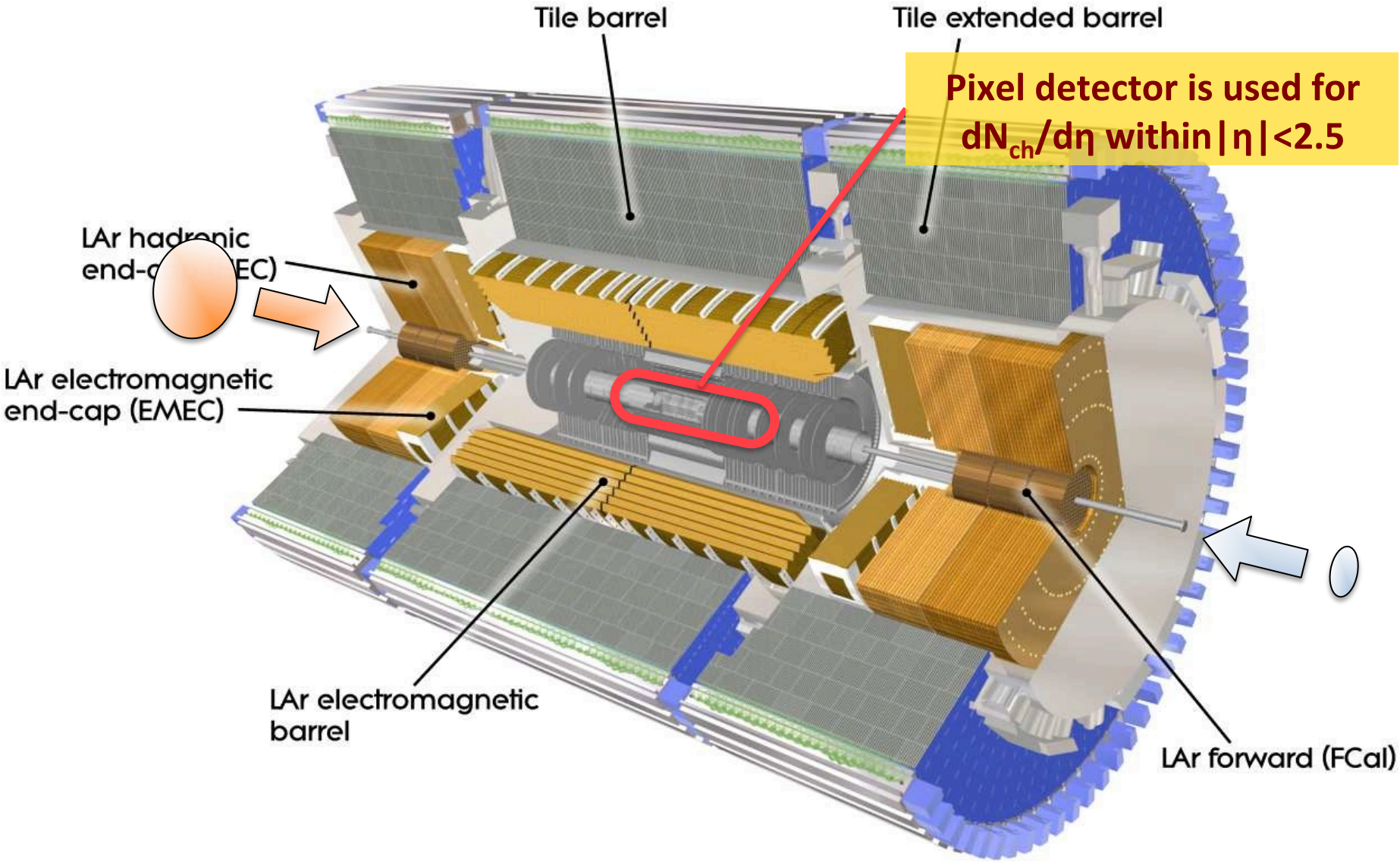

p+Pb @ LHC and ATLAS

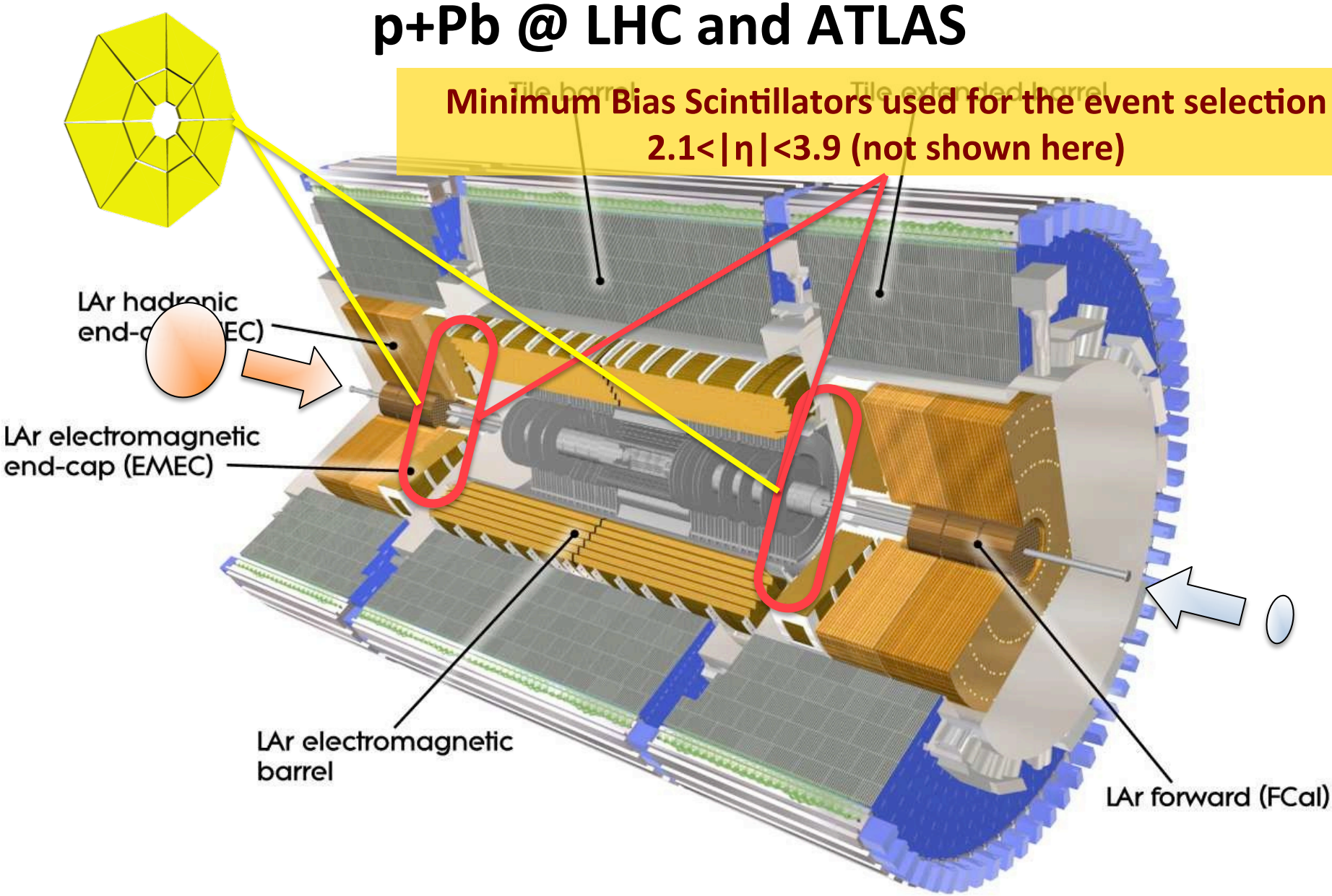

p+Pb @ LHC and ATLAS

All calorimeters are used for the diffraction contribution studies |η|<4.9

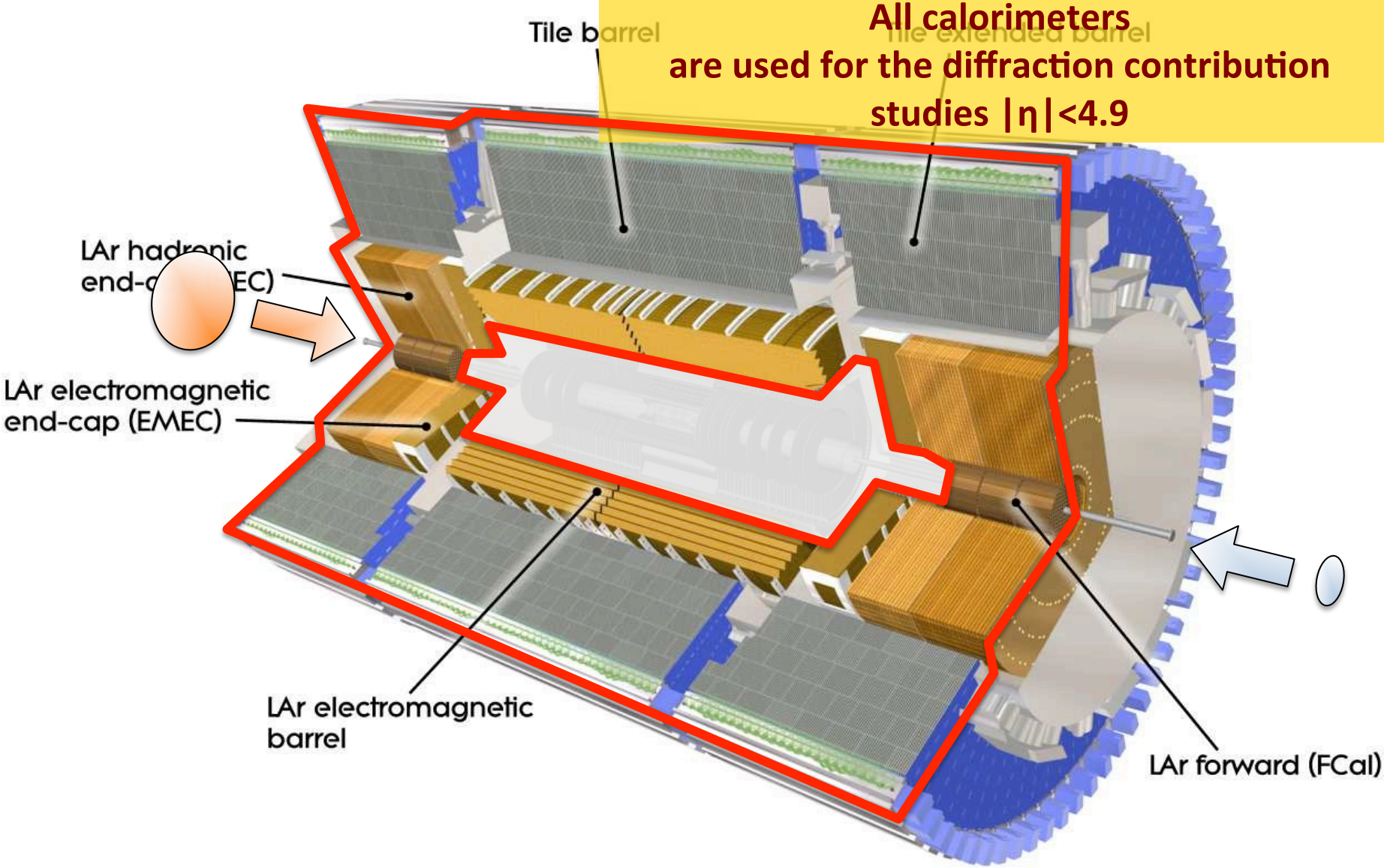

p+Pb @ LHC and ATLAS

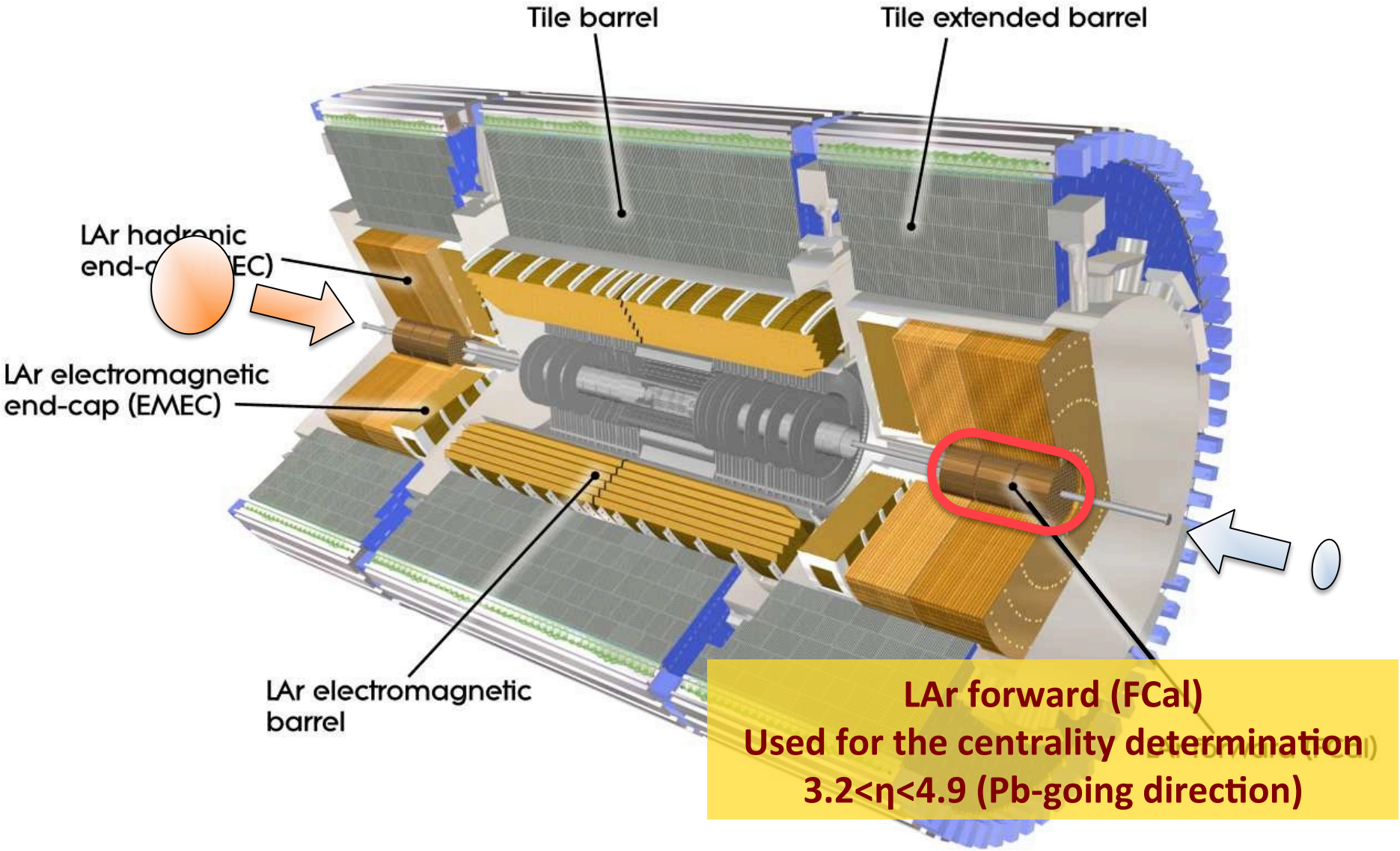

Event selection

2012 p+Pb pilot run is used for the measurements
Integrated Luminosity: $1\mu b^{-1}$

1. Two scintillator signals in the MBTS:
2. Good timing $|\Delta t|<10$ns

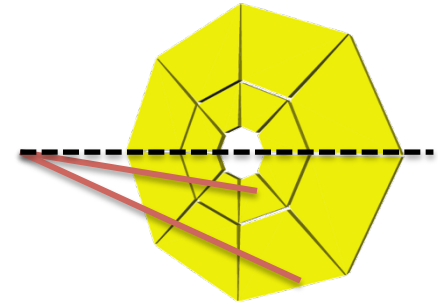

3. Reconstructed vertex with at least two tracks of $p_T>100$ MeV.

4. Pileup during data taking was at the level of 10^{-3}
5. Events with two good vertices were rejected, residual pile-up 10^{-4}

6. A pseudorapidity gap on the lead going side of $\Delta\eta^{Pb}\leq 2.0$

Sample used in the analysis: 2,131,219 events.
This sample corresponds to 98±2% of the inelastic events.

Removal of events with large η gaps

- pPb interactions produce an additional coherent and photo-nuclear component of events consistent with the excitation of the proton

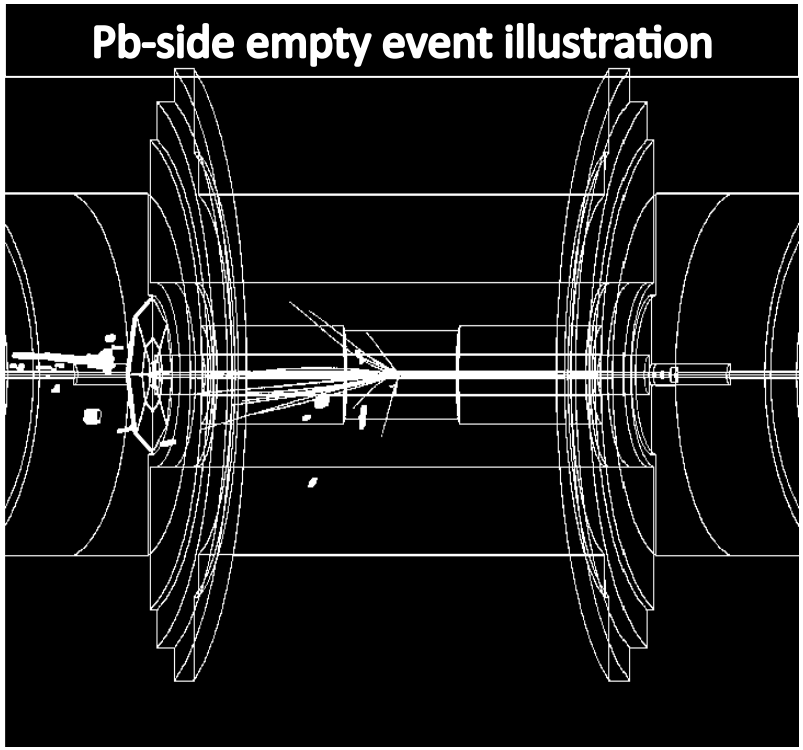

- Full coverage $|\eta| < 4.9$ divided into $\Delta\eta = 0.2$ intervals
- Occupied interval , contains reconstructed tracks or calorimeter clusters with $p_T > 200$ MeV
- $\Delta\eta^{Pb}_{gap} = \Sigma\Delta\eta^{Pb}_{Empty\ interval}$
- Electromagnetic or diffractive excitation of the proton typically produce $\Delta\eta^{Pb}_{gap} > 2$ ($f_{gap} = 6\%$)

Centrality definition

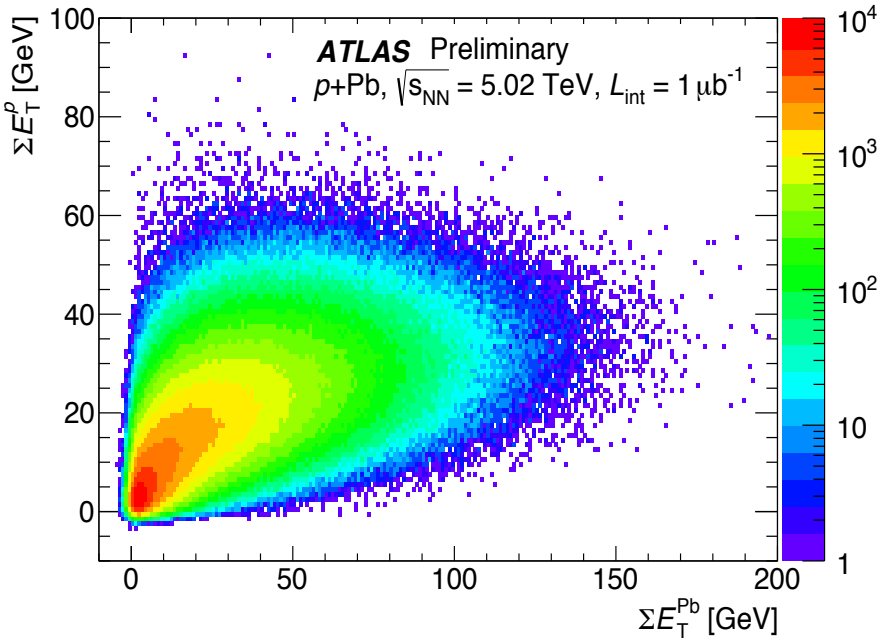

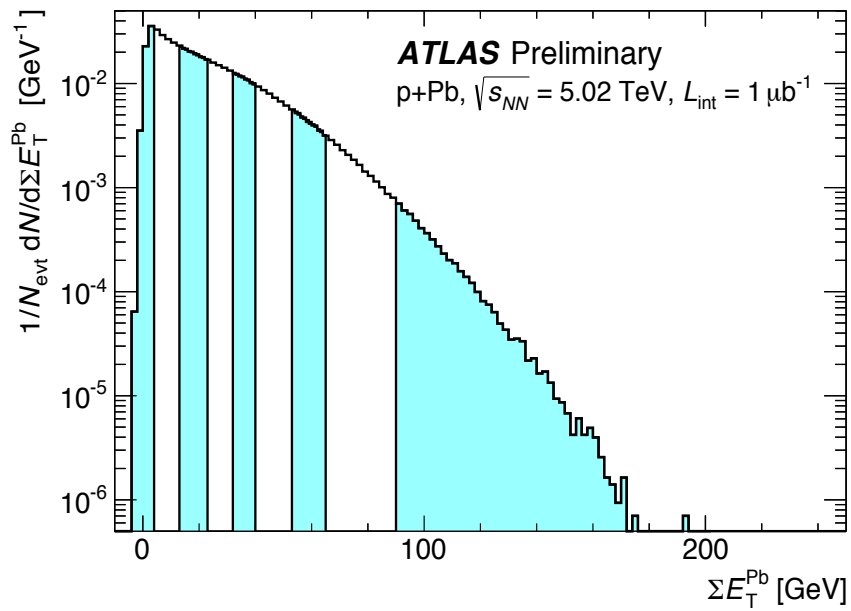

- Pb-going FCal (side "A") is used to characterize event centrality, it is more sensitive to nuclear geometry
- FCal ΣE^{Pb}_T is divided into centrality intervals: 0-1%, 1-5%, 5-10%, 10-20%, 20-30%, 30-40%, 40-60%, 60-90%
- 90-100% is excluded due to larger systematic uncertainties on event composition and reconstruction efficiency

Glauber and Glauber-Gribov models

To model Npart distribution we used:

- standard Glauber with σ_{NN} cross section = 70±5mb
- Glauber-Gribov color fluctuation models, with $\langle\sigma_{NN}\rangle$ cross section = 70±5mb

In Glauber-Gribov model:

- σ_{tot} is considered frozen for each event
- parameter Ω controls the amount of fluctuations
- Ω is extracted from experimental data: 0.55 [PLB633 (2006) 245–252] and 1.01 [PLB 722 (2013) 347–354]

$$P_h(\sigma_{tot}) = \rho \frac{\sigma_{tot}}{\sigma_{tot}+\sigma_0} \exp\left\{-\frac{(\sigma_{tot}/\sigma_0 - 1)^2}{\Omega^2}\right\}. \qquad P_H(\sigma_{NN}) = \frac{1}{\lambda} P(\sigma_{NN}/\lambda)$$

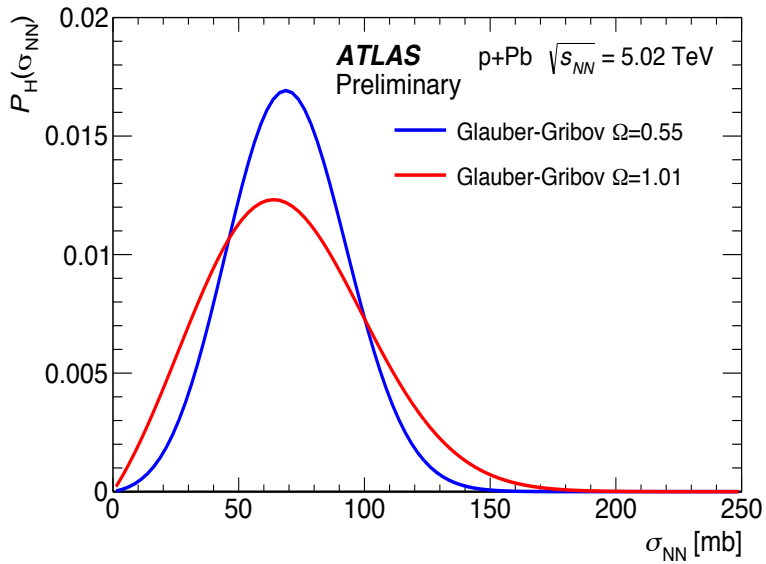

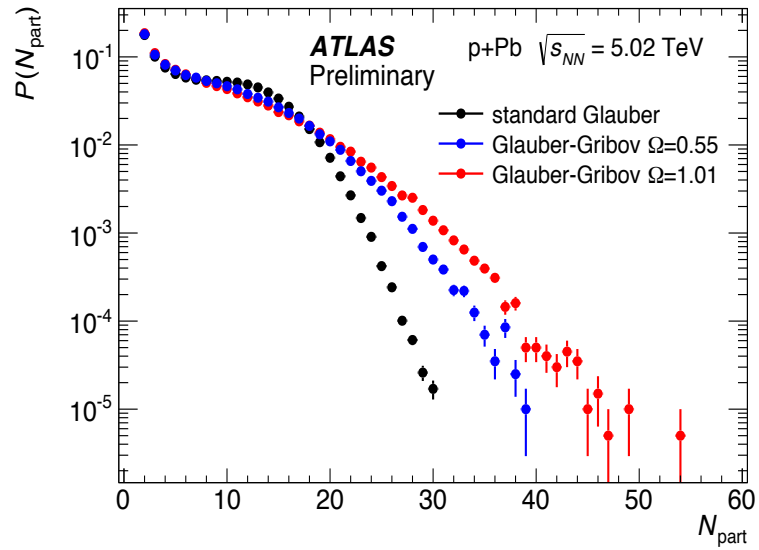

Constructing FCal ΣE_T^{Pb} response

E_T distribution modeled by PYTHIA simulated taking into account FCal response in p +Pb configuration and were approximated by Gamma(k,θ) distributions

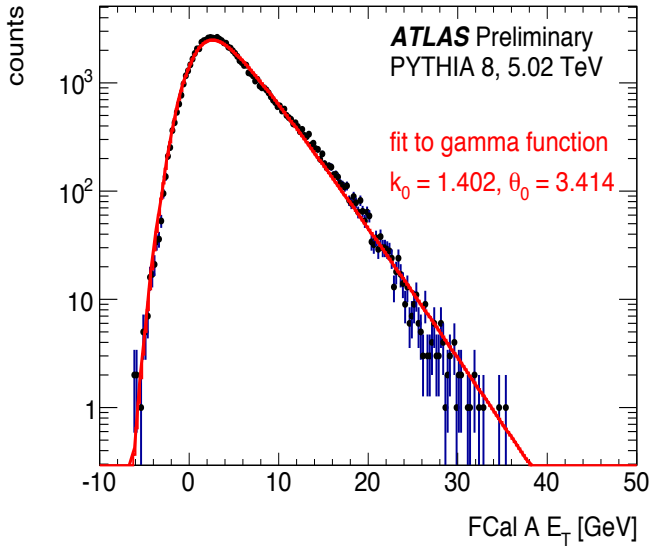

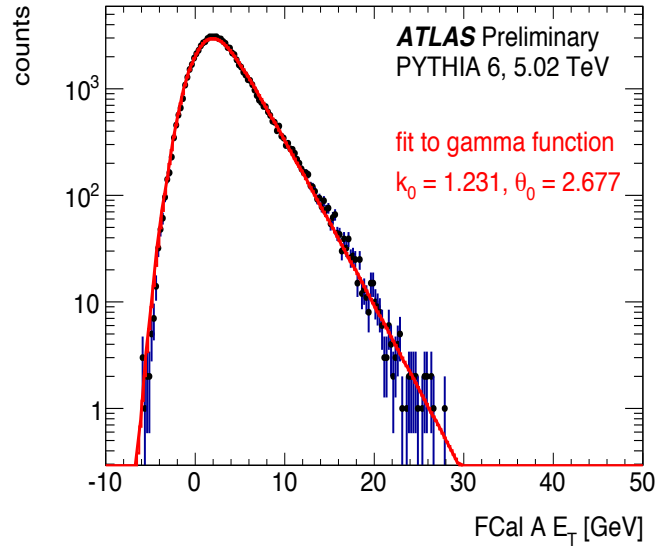

Convolution of N_{part} Gamma(k,θ) was taken as Gamma($k(N_{part})$,$\theta(N_{part})$)

We allowed: $k(N_{part}) = k_0+k_1*(N_{part}-2)$; $\theta(N_{part}) = \theta_0+\theta_1*(\log(N_{part}-1))$;

In WN : $k(N_{part}) = k*N_{part}$; $\theta(N_{part}) = \theta$;

E_T response for N_{part} was weigthed according to Glauber or Glauber-Gribov model and fitted to the data

FCal E_T distribution fits

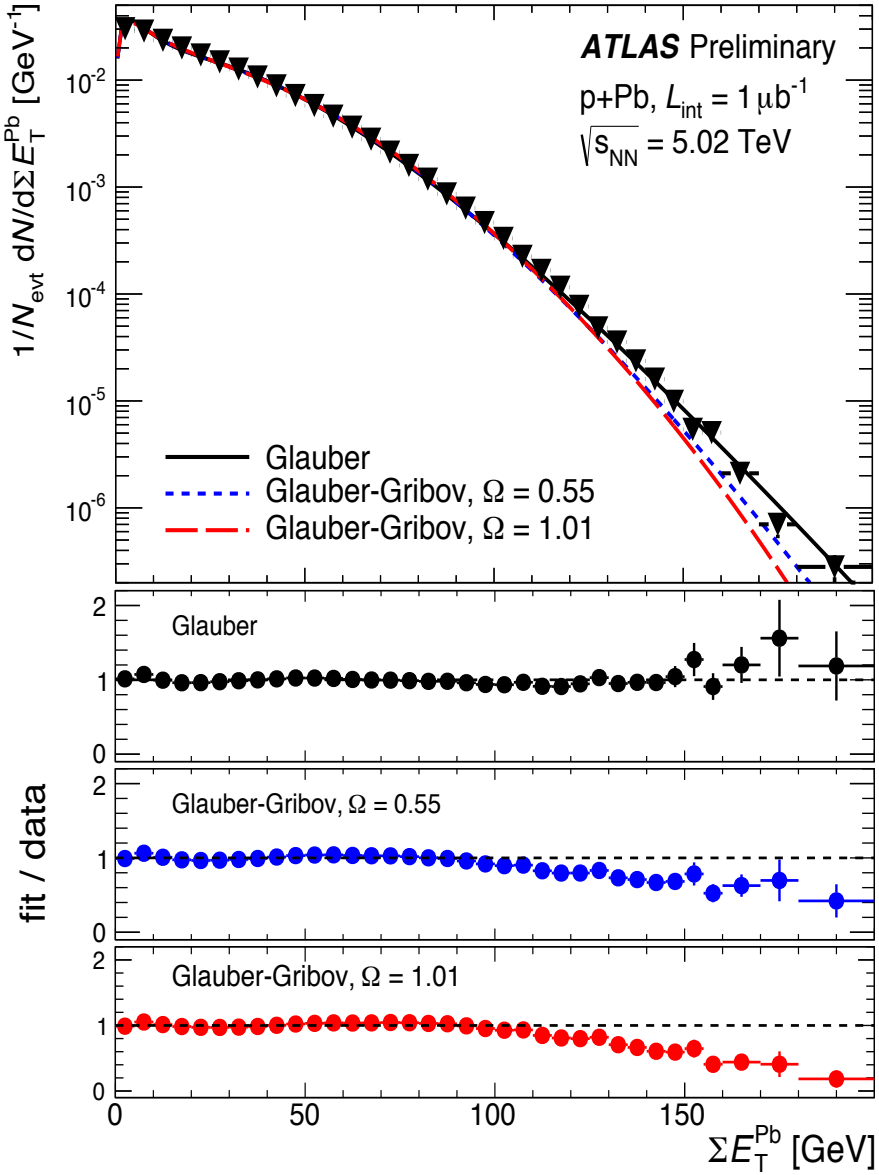

- dN_{evt}/dE_T obtained by summing the gamma distributions over different N_{part} values weighted by $P(N_{part})$

Fits to the measured E^{Pb}_T distributions show reasonable agreement over 3 orders of magnitude in E_T distribution.

N_{part} for different Glauber models

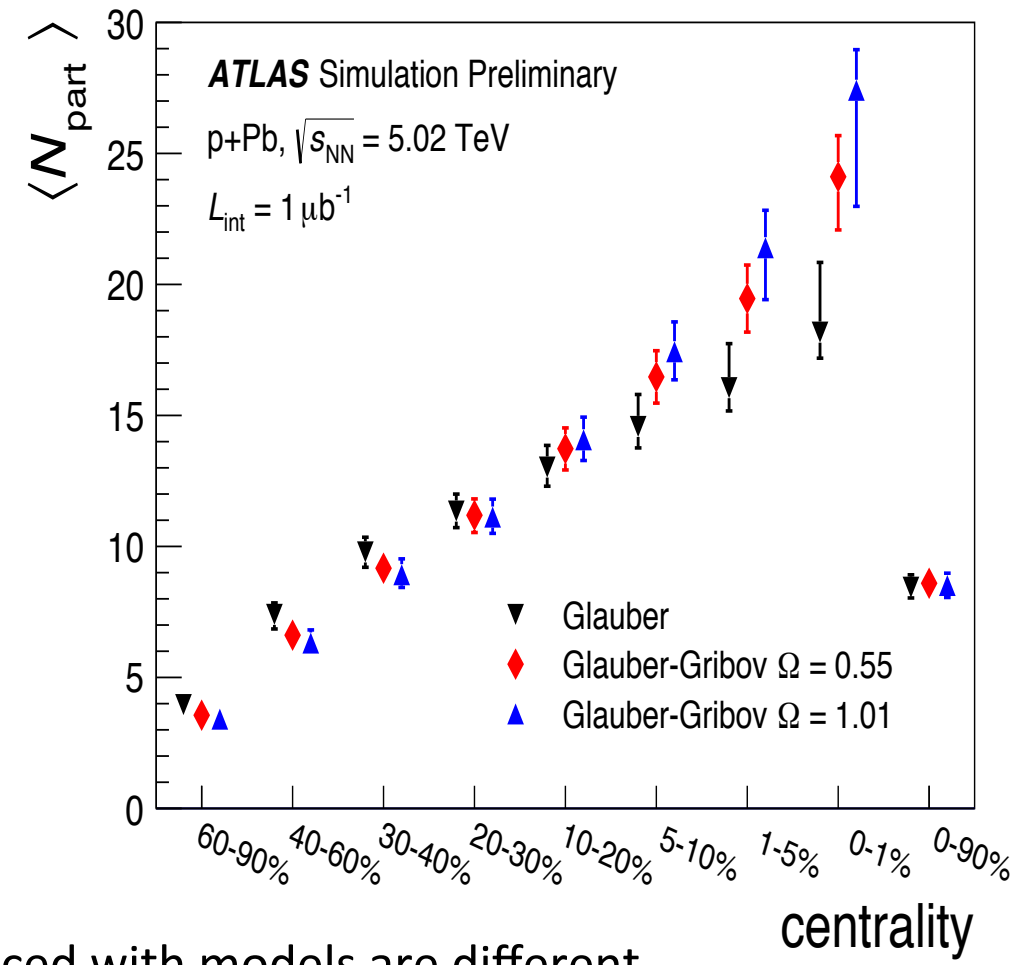

- Results produced with models are different
- Standard Glauber has highest fluctuations of produced E_T per participant
- Glauber-Gribov Ω=1.01 has less E_T fluctuation and therefore gives highest N_{part}

$dN_{ch}/d\eta$ measurement

Multiplicity Analysis

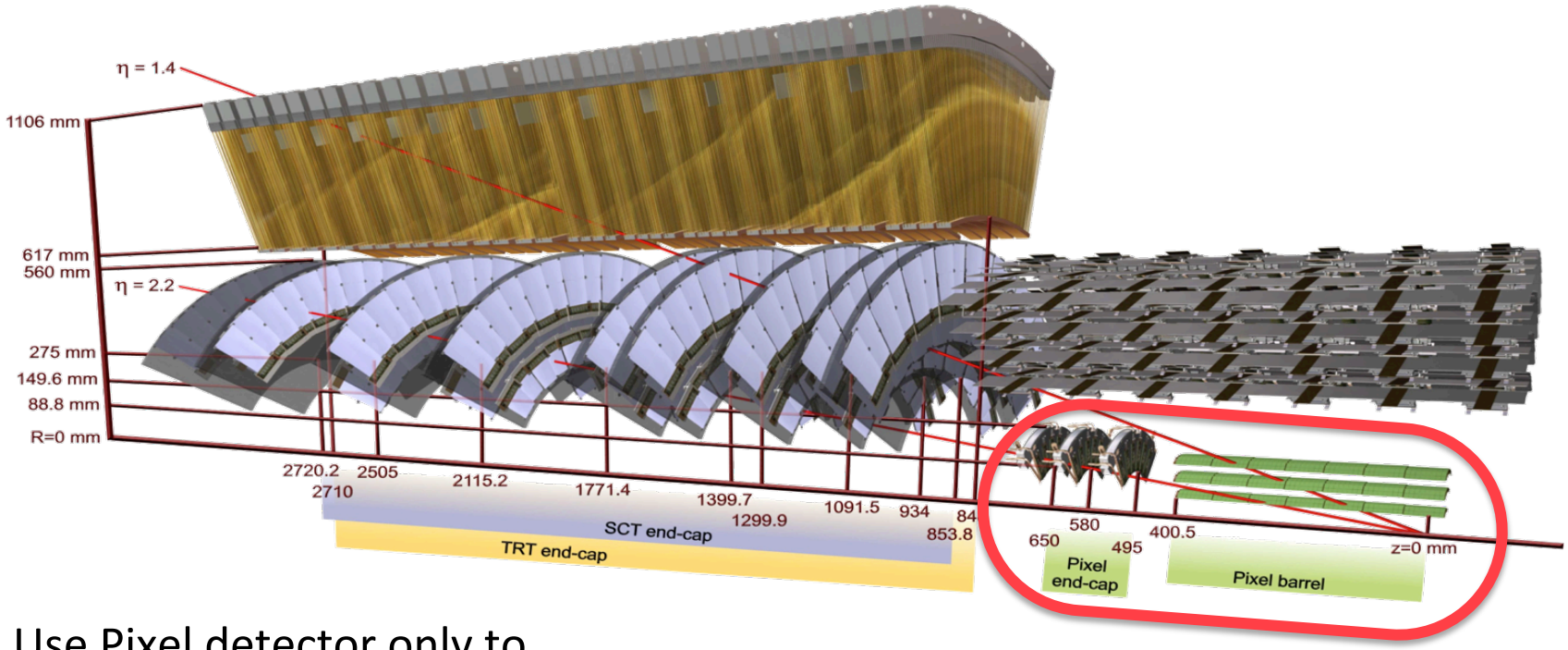

- Use Pixel detector only to
  have largest acceptance at low p_T of registered particles

- Three analysis methods used in parallel to control combinatorial background
  Standard pixel tracks: lower acceptance, low fakes
  Tracklet method 1: largest acceptance, some fakes
  Tracklet method 2: large acceptance, more fakes, with fake rate estimate

Three Analysis Methods

Pixel tracks:

- $|\eta|<2.5$
- provide p_T of the particle
- used to reweight HIJING -> Data

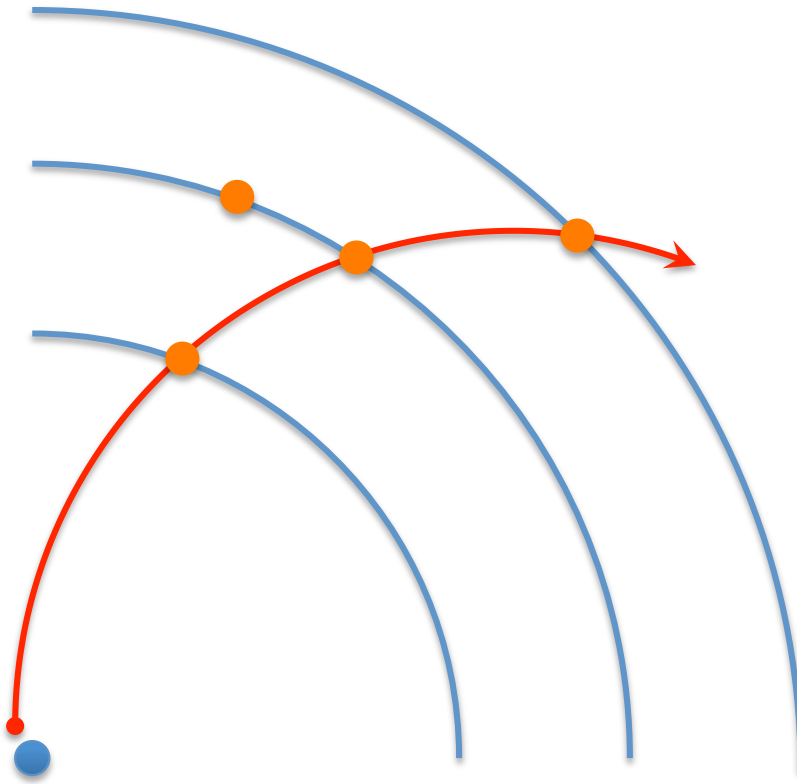

Two Tracklet Methods

Method 1

tracklet = Vertex + 2 hits/clusters

- only one tracklet for a given cluster on the first pixel layer.
- for multiple clusters on the second pixel layer, two tracklets merged into a single
- method limits but do not suppress fake tracks

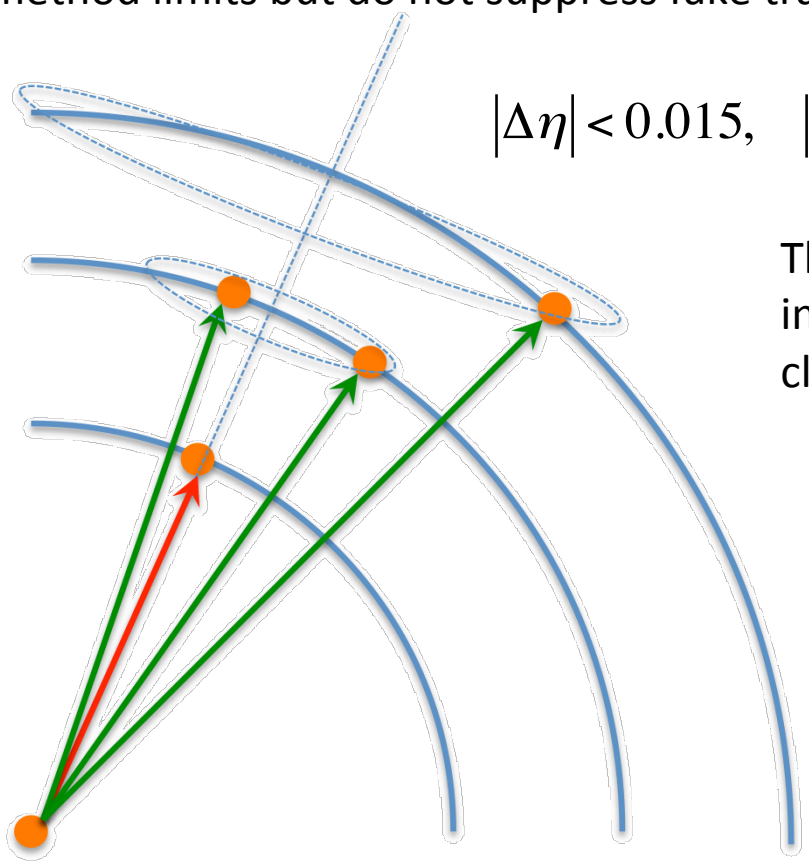

$$|\Delta\eta| < 0.015, \quad |\Delta\varphi| < 0.1, \quad |\Delta\eta| < |\Delta\varphi|$$

The primary event vertex and clusters on an inner pixel layer define a search region for clusters in the outer layers

Two Tracklet Methods

Method 2

- reconstructed tracklets for all combinations of clusters in only two pixel layers
- fake tracklets arising from random combinations of clusters, obtained with inverting the X and Y positions of all clusters on the second layer with respect to the primary vertex

$$|\Delta\eta| < 0.015, \quad |\Delta\varphi| < 0.1, \quad |\Delta\eta| < |\Delta\varphi|$$

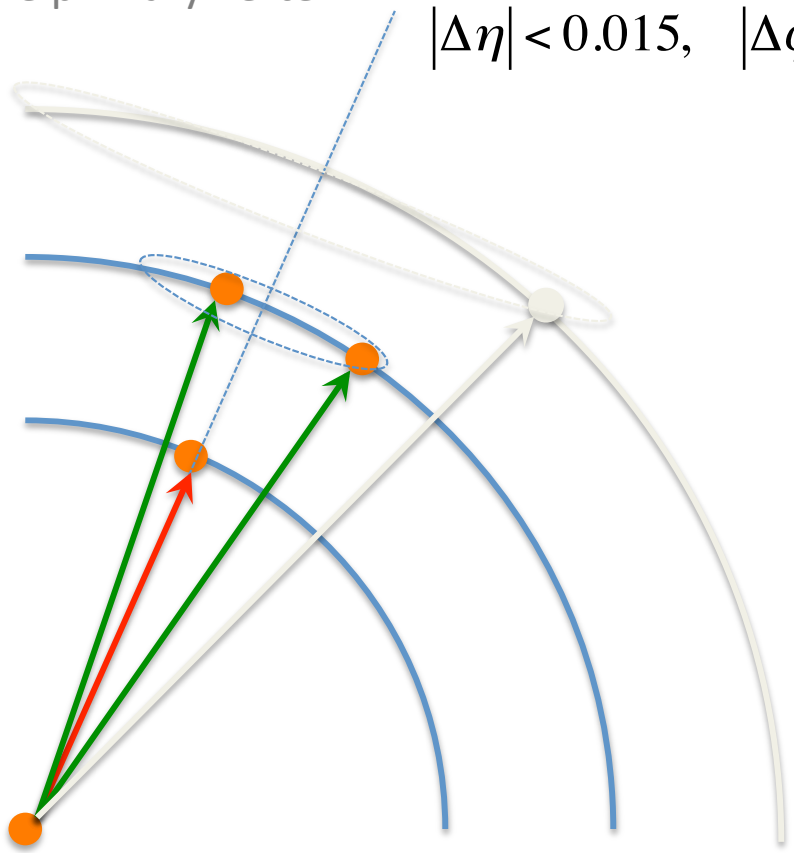

Two Tracklet Methods

Method 2

- reconstructed tracklets for all combinations of clusters in only two pixel layers
- fake tracklets arising from random combinations of clusters, obtained with inverting the X and Y positions of all clusters on the second layer with respect to the primary vertex

$$|\Delta\eta| < 0.015, \quad |\Delta\varphi| < 0.1, \quad |\Delta\eta| < |\Delta\varphi|$$

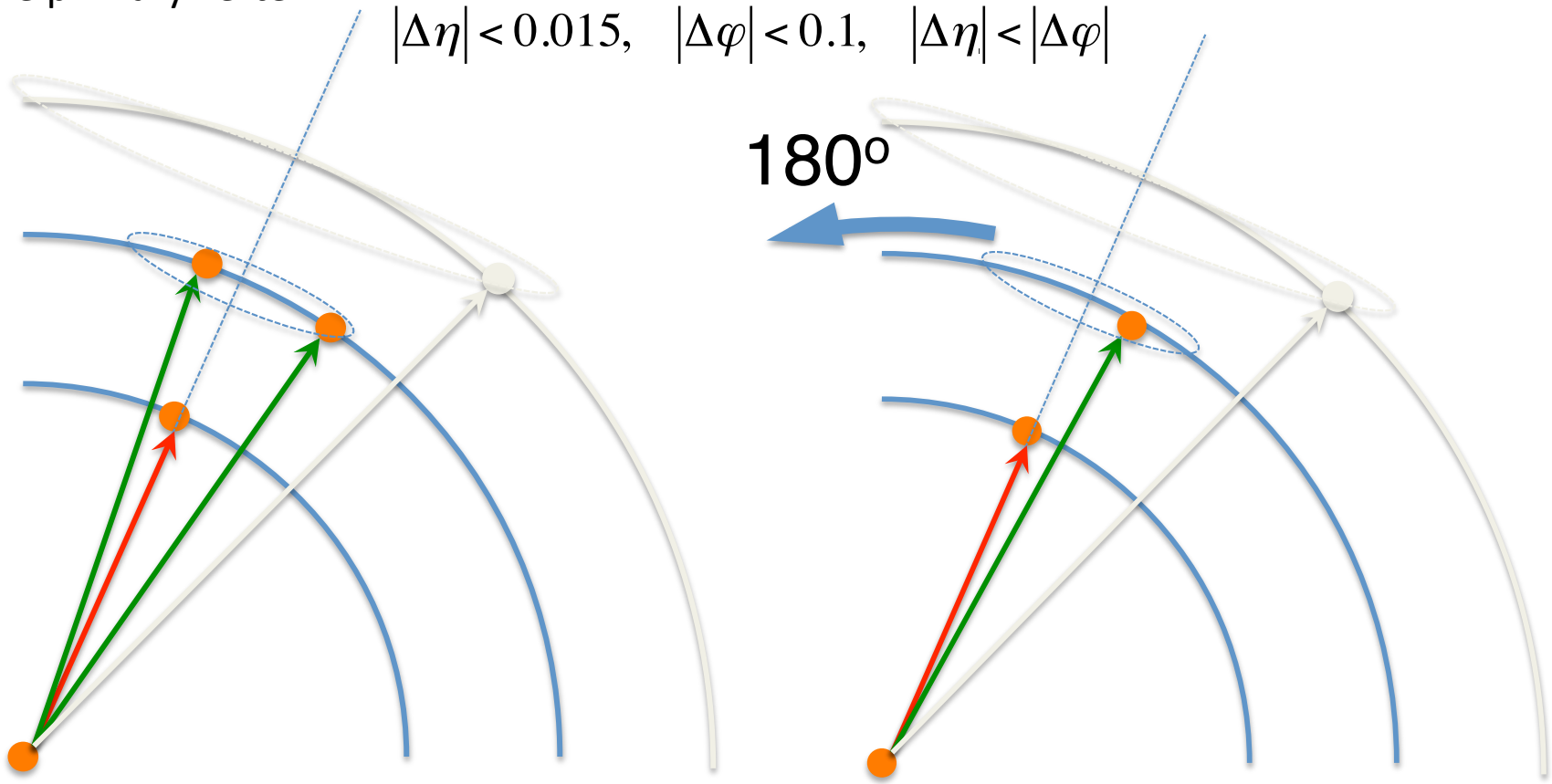

Fake tracklets estimation

- Method 2 has the largest contribution of fakes
- The results are in good agreement with each other -> fake rejection and the correction procedure are well understood

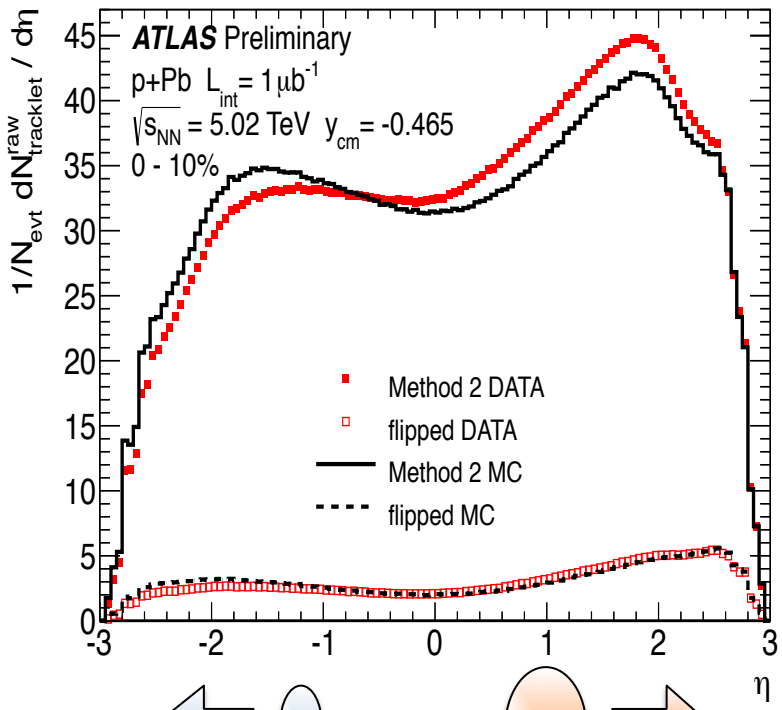

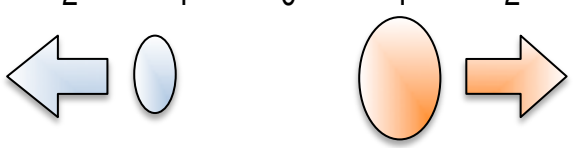

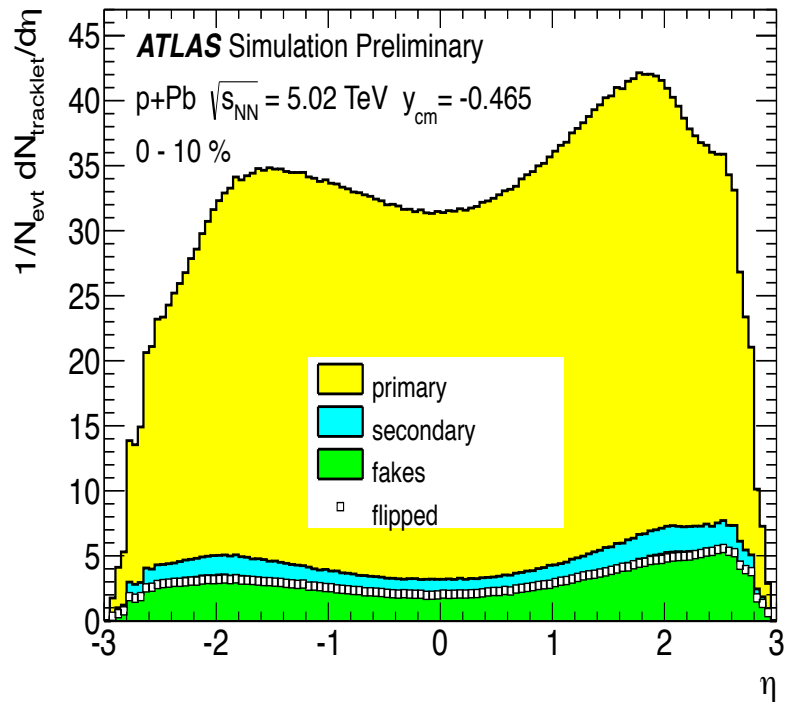

Corrections provided by three methods

- Method 1 is chosen as the default result for $dN_{ch}/d\eta$
- Method 2 is used for systematic uncertainties
- Pixel track method is used primarily as a consistency test
- The correction factor is evaluated as a function of occupancy (O), event vertex (z_{vtx}), and η as:

$$C(O, z_{vtx}, \eta) \equiv \frac{N_{pr}(O, z_{vtx}, \eta)}{N_{rec}(O, z_{vtx}, \eta)},$$

$$\frac{dN_{ch}}{d\eta} = \frac{1}{N_{evt}} \sum_{\nu} \frac{\Delta N^{raw}(O, z_{vtx}, \eta) C(O, z_{vtx}, \eta)}{\Delta\eta},$$

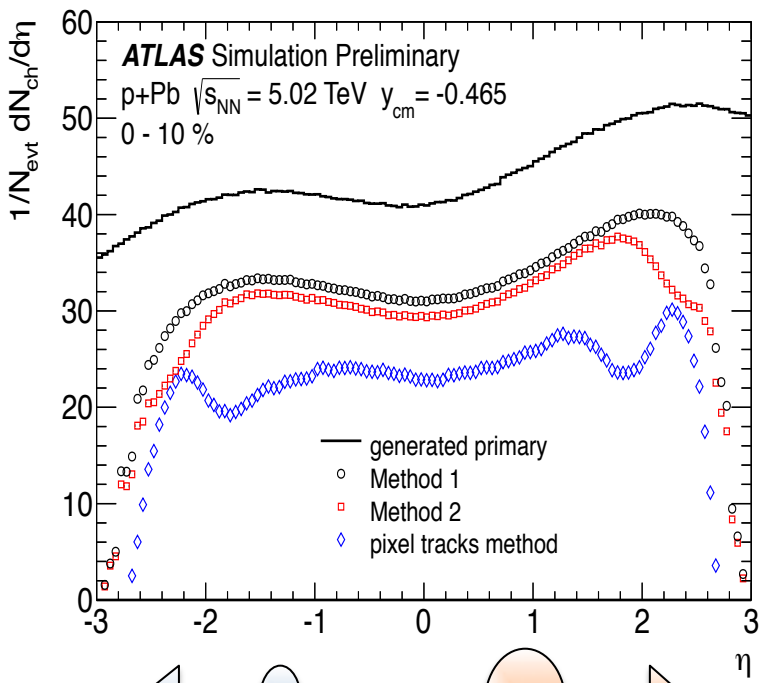

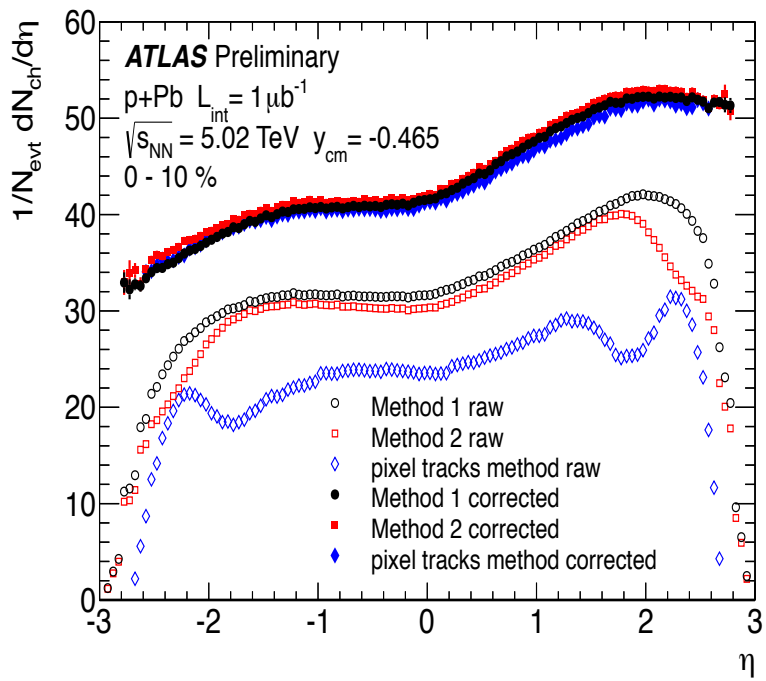

Systematic Uncertainties

Sources of uncertainties:

- inaccuracies of detector description in simulations
- sensitivity to selection criteria, including fakes and secondaries
- differences between data and MC

To extract uncertainties for each source, one of the parameters used in the analysis, such as tracklets selection criteria, simulated particle composition, etc. was altered within acceptable limits.

	Uncertainty 60-90%		Uncertainty 0-1%	
Source	barrel	endcap	barrel	endcup
MC detector description	1.7%		1.7%	
Extra material	1%	2%	1%	2%
Tracklet selection	0.5%	1.5%	0.5%	1.5%
p_T re-weighting	0.5%	0.5%	0.5%	3.0%
Extrapolation to p_T=0	1%	2.5%	1%	2%
Particle composition	1%		1%	
Analysis method	1.5%	2.0%	1.5%	2.5%
Event selection	5.0%	6.0%	0.5%	0.5%

dN/dη for different centralities

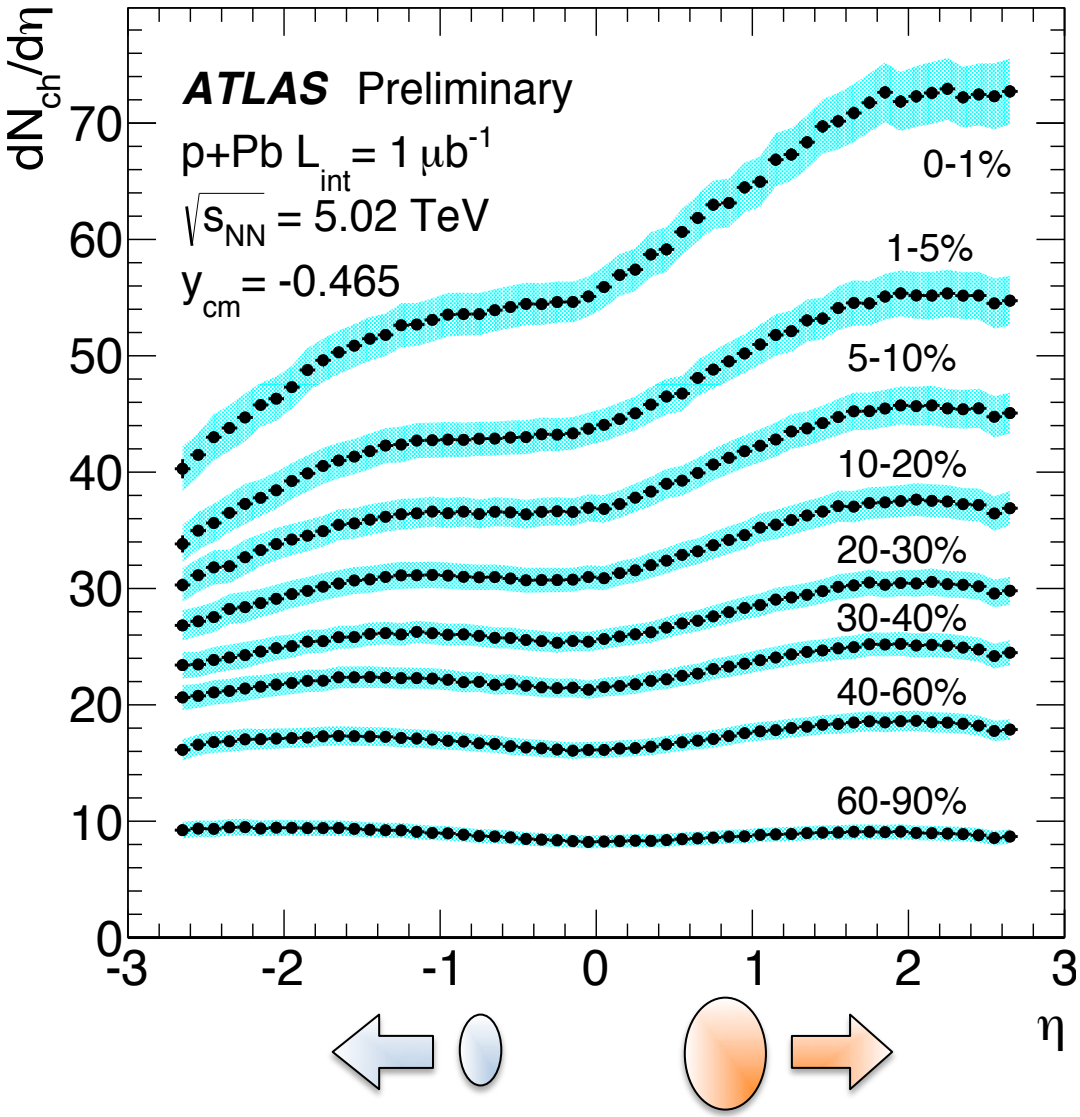

- $dN_{ch}/d\eta$ is measured for $|\eta| < 2.7$ in eight centrality intervals
- 60-90% - double-peak structure similar to pp
- Forward backward asymmetry between p and Pb going directions grows with centrality

dN/dη for different centralities

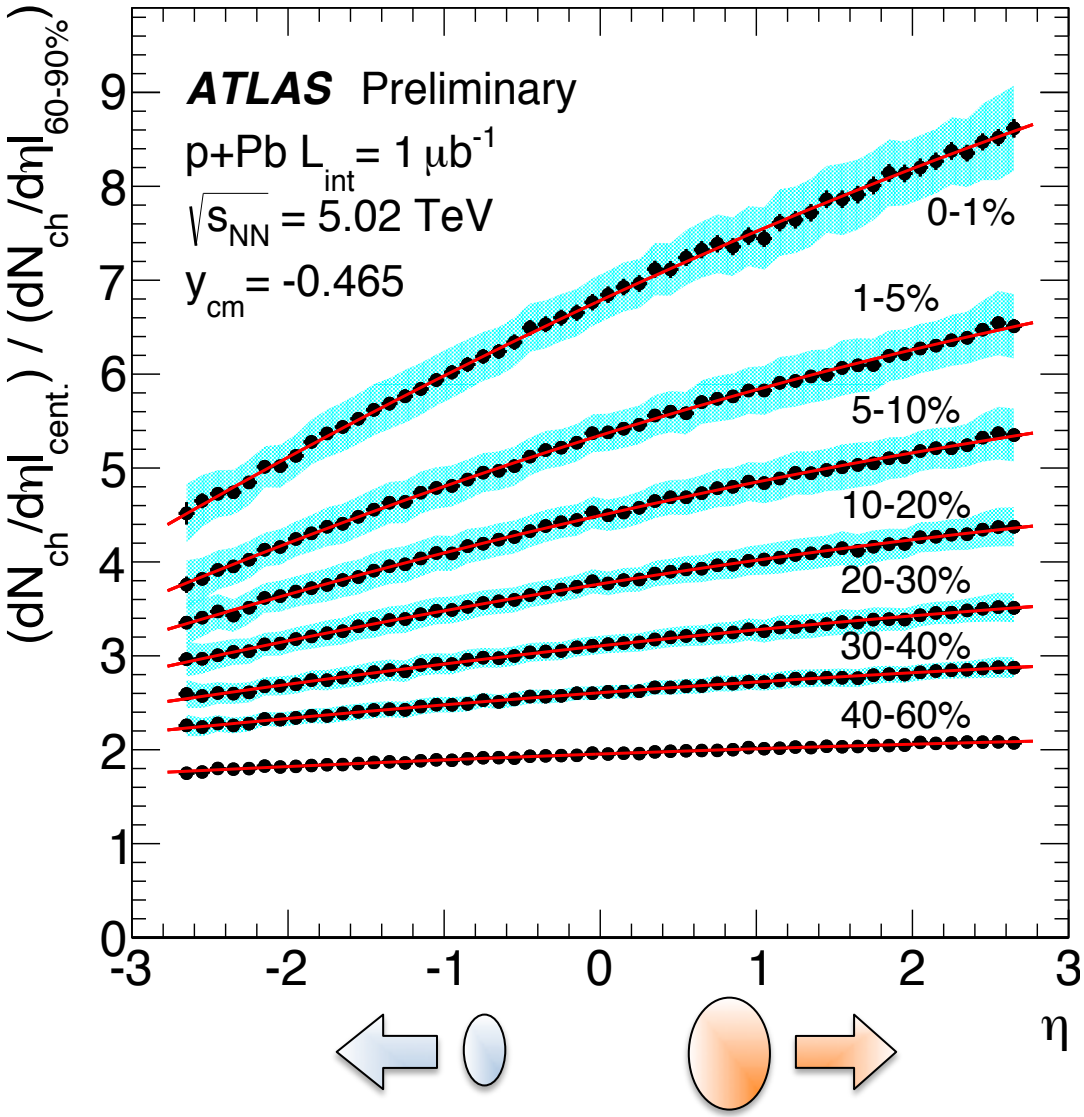

- $dN_{ch}/d\eta$ ratios to 60-90% is measured for $|\eta| < 2.7$ in seven centrality intervals
- Almost linear distributions fitted with 2-nd order polynomial
- double-peak structure disappears as it have been provided by kinematics of the events
- 0-1% grows ~2 times from p- to Pb-going direction

Centrality dependence of $\langle dN_{ch}/d\eta \rangle$

- $\langle dN_{ch}/d\eta \rangle$ per pair of participants vs N_{part} for five η intervals
- Results are dependent on Glauber implementation
- Standard Glauber, used up to now shows increase with $\langle N_{part} \rangle$
- Glauber-Gribov with Ω=0.55 is almost flat with Ω=1.01 even decreases

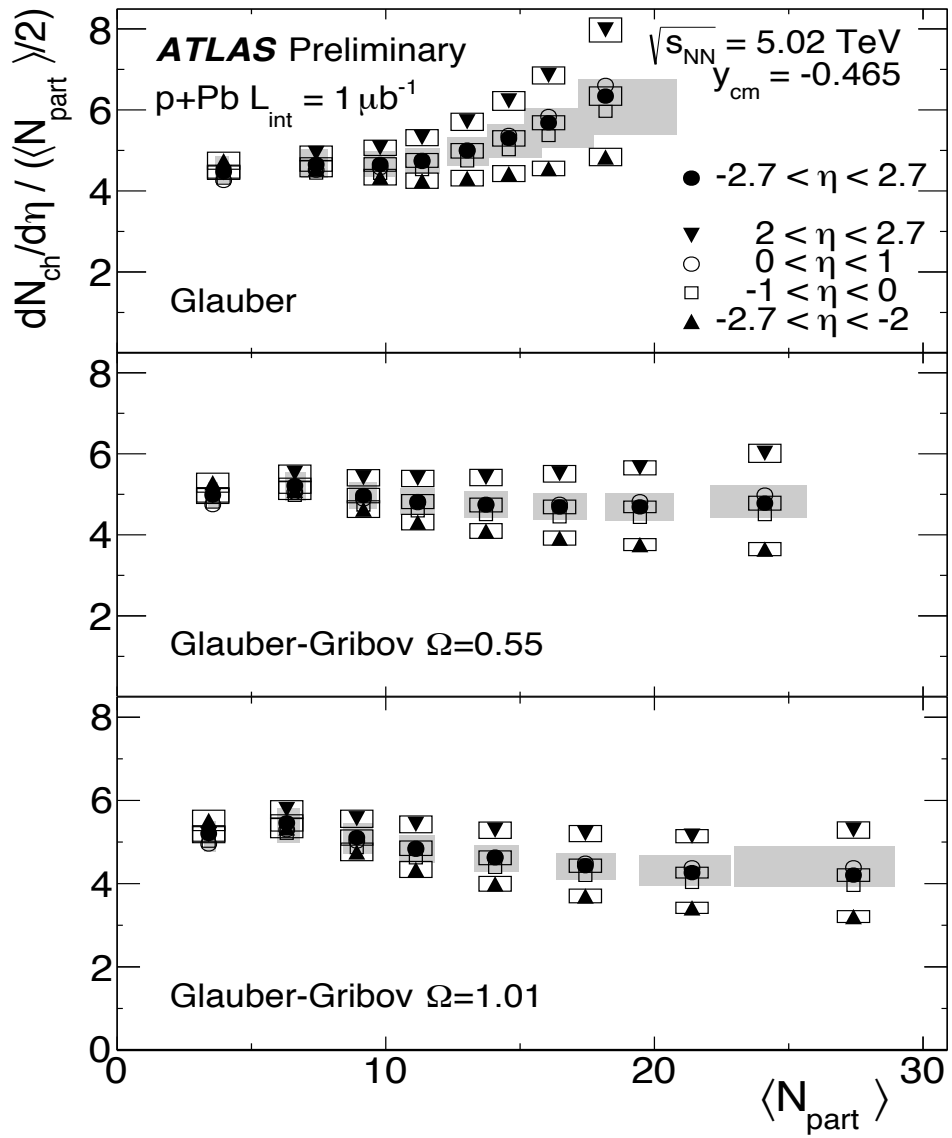

Glauber models comparison

- $dN_{ch}/d\eta$ per pair of participants for two centrality bins and three Glauber models
- Strong correlation of the results with the model
- These results point to the importance of understanding not just the initial state of the nuclear wave function, but also the fluctuating nature of nucleon-nucleon collisions themselves

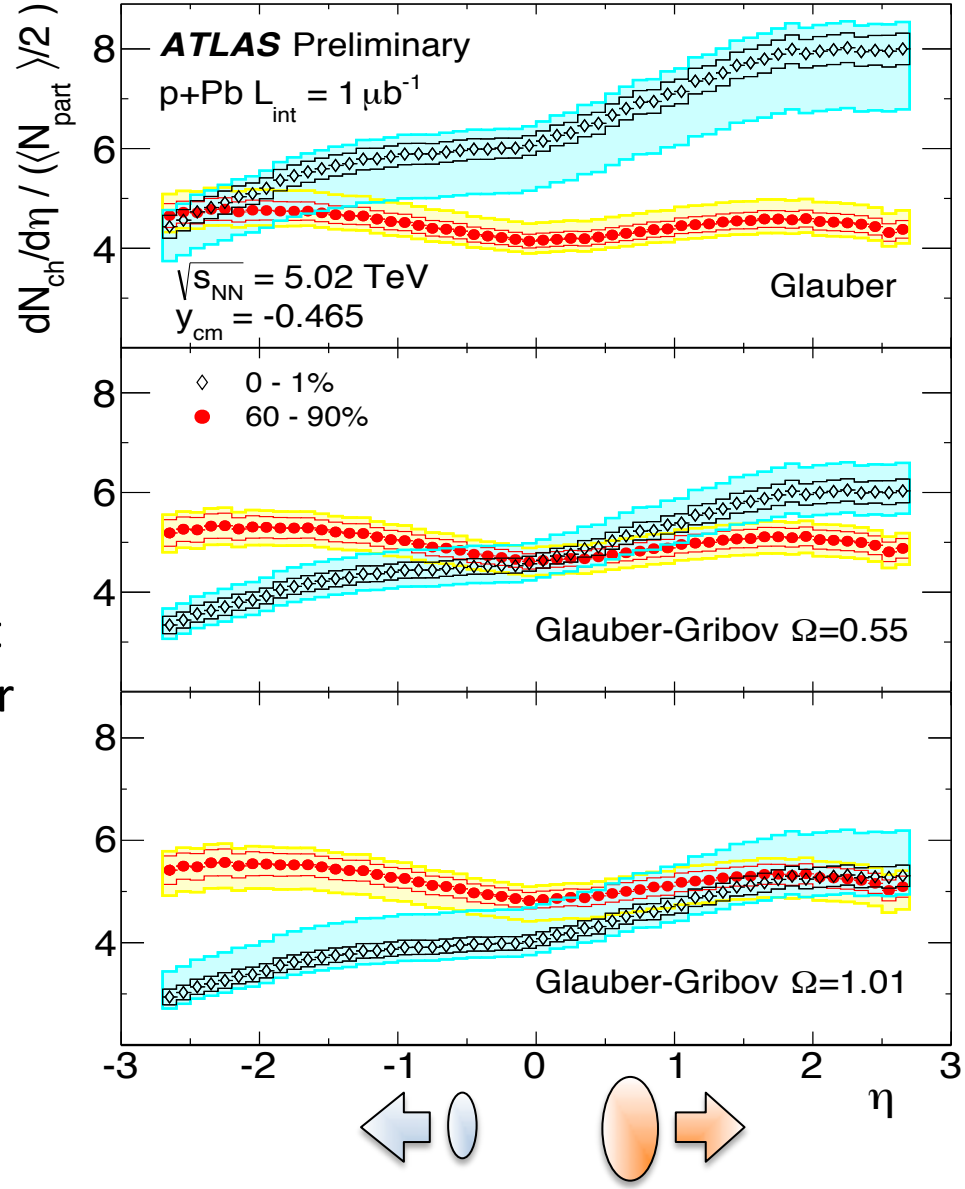

Conclusion

- ATLAS measurements of the centrality dependence of the charged particle pseudorapidity distribution, $dN_{ch}/d\eta$ in p+Pb collisions at a nucleon-nucleon center-of-mass energy of $\sqrt{s_{NN}}$ = 5.02 TeV over the $|\eta|<2.7$ range with a $y_{c.m.s.}$=-0.465 are presented for 8 centrality classes and for the 90% most central p+Pb collisions

- Collision centrality definition performed using a forward calorimeter covering $3.2 < \eta < 4.9$ in the lead-going direction

- Performed the average number of participants in each centrality interval, $\langle N_{part} \rangle$, estimated using a Monte Carlo Glauber model as well as in a Glauber-Gribov approach

- It have been shown that centrality dependence of $dN_{ch}/d\eta/(\langle Npart \rangle/2)$ is sensitive to the Glauber modeling

- Performed results point to the importance of understanding not just the initial state of the nuclear wave function, but also the fluctuating nature of nucleon-nucleon collisions themselves.

Thank you for attention!

High multiplicity p+Pb event

Event Display

Run: 217946
Event: 32291041
Date: 2013-01-20

N_{Trk} (p_T > 0.4 GeV) = 273,
N_{Trk} (p_T > 1.0 GeV) = 106 (shown)
FCal A (Pb going side) ΣE_T = 139 GeV

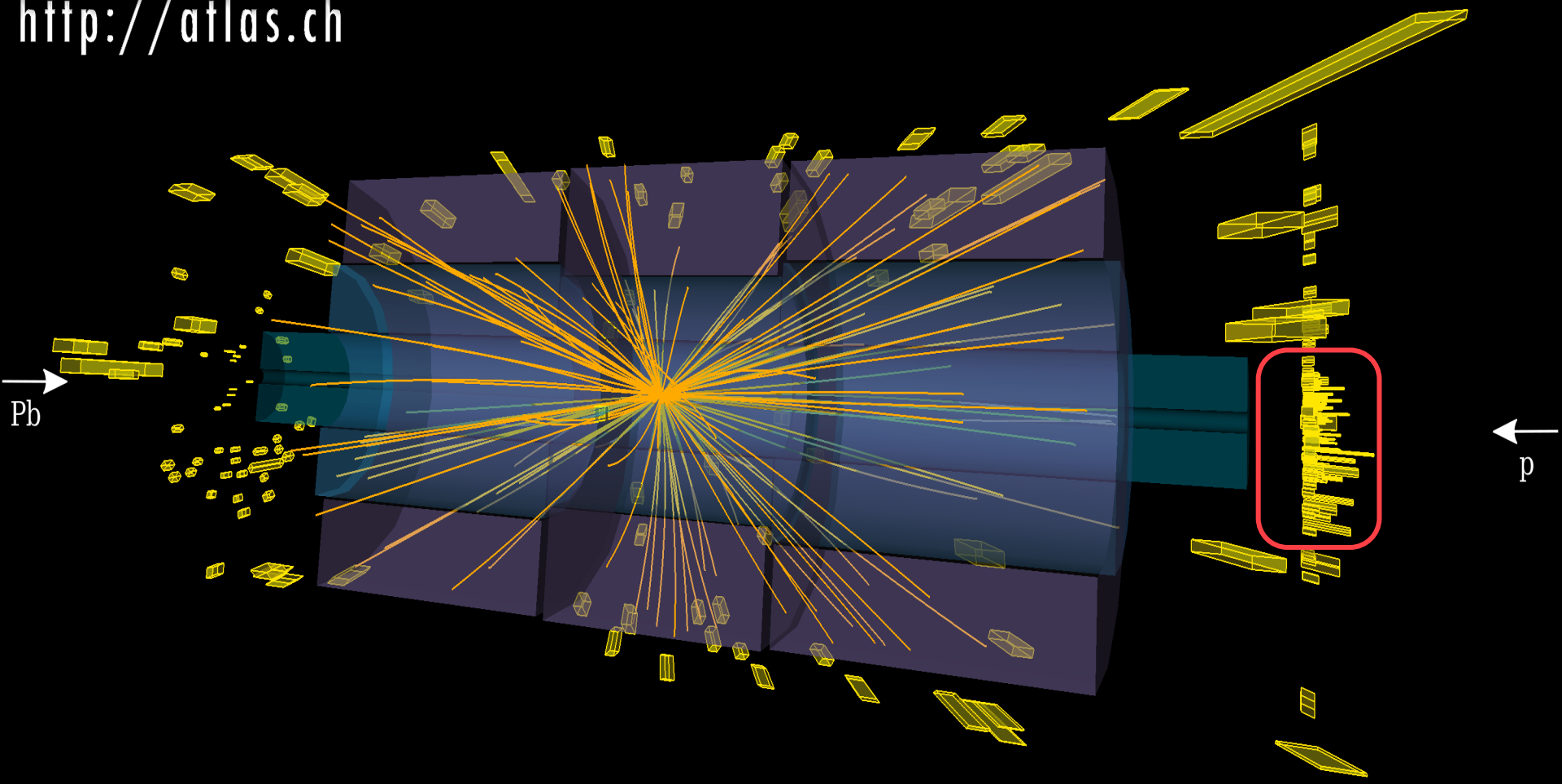

Removal of events with large η gaps

- Additional diffraction component (coherent and photo-nuclear) consistent with the diffractive excitation of the proton have to be subtracted

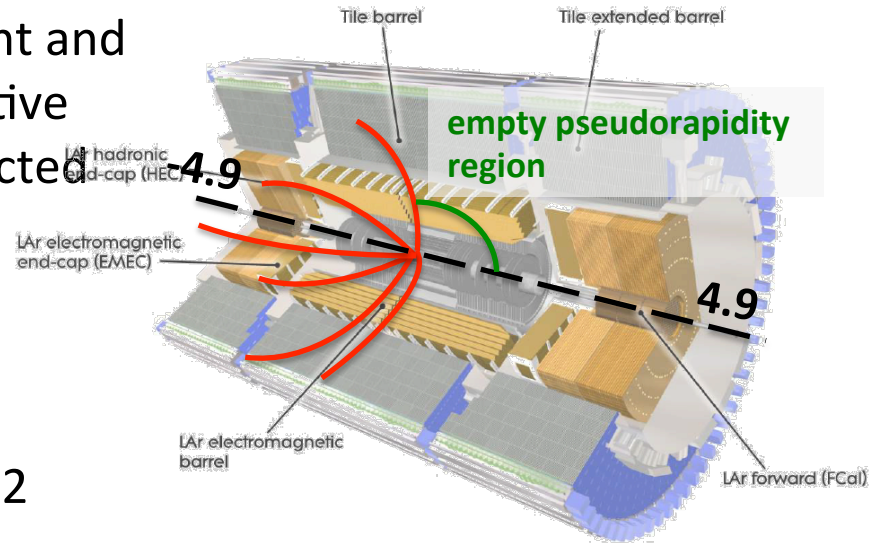

- Estimation of the additional diffraction component relies on previous pp studies
- Full coverage $|\eta| < 4.9$ divided into $\Delta\eta = 0.2$
- $\Delta\eta^{Pb}_{gap}$ edge-gap - distance between the detector edge on the Pb-going side and the nearest occupied interval, containing reconstructed tracks or calorimeter clusters with p_T > 200 MeV.
- Electromagnetic or diffractive excitation of the proton typically produce $\Delta\eta^{Pb}_{gap}>2$ (f_{gap} = 6%)

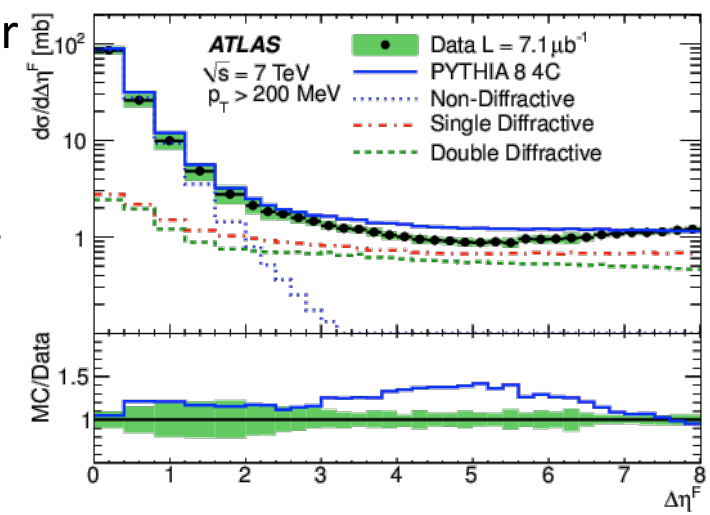

Eur. Phys. J. C72 1926

Δη and Δϕ distributions for tracklets

- All three methods rely on the MC to correct for secondary particles
- Method 1 and the pixel track method rely on the MC to correct for fakes

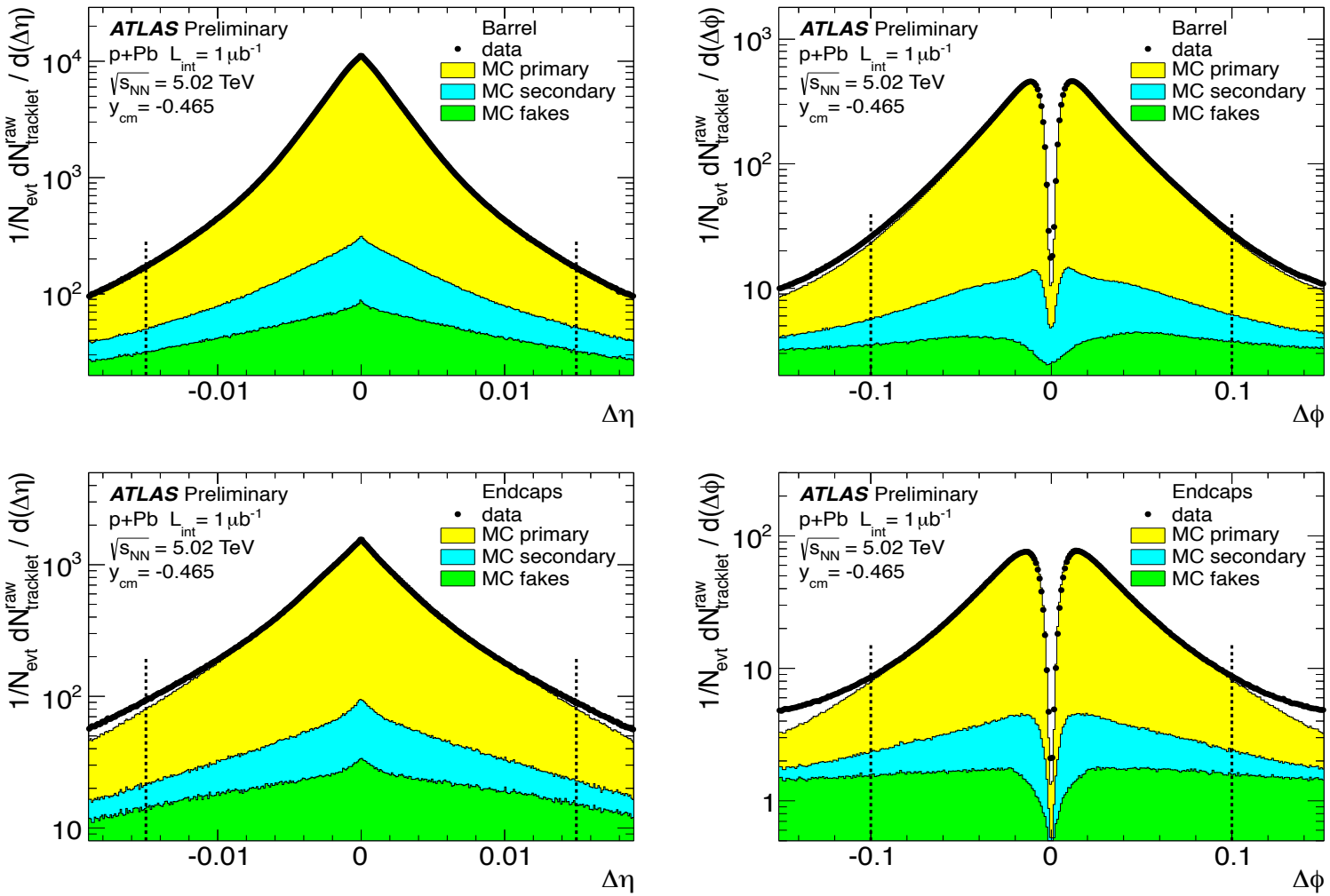

pol2 fit parameters

Centrality ratio	c	b	a
0 - 1% / 60 - 90%	6.78±0.28	0.77±0.05	-0.033±0.006
1 - 5% / 60 - 90%	5.35±0.22	0.515±0.031	-0.030±0.005
5 - 10% / 60 - 90%	4.49±0.18	0.377±0.021	-0.0218±0.0035
10 - 20% / 60 - 90%	3.77±0.14	0.269±0.014	-0.0169±0.0025
20 - 30% / 60 - 90%	3.11±0.11	0.182±0.010	-0.0113±0.0020
30 - 40% / 60 - 90%	2.61±0.08	0.122±0.006	-0.0076±0.0016
40 - 60% / 60 - 90%	1.95±0.06	0.0595±0.0031	-0.0037±0.0011

N_{part} values

Centrality	Glauber	Glauber-Gribov $\Omega = 0.55$	Glauber-Gribov $\Omega = 1.01$
60-90%	$3.96^{+0.20}_{-0.31}\left(^{+5\%}_{-8\%}\right)$	$3.56^{+0.19}_{-0.17}\left(^{+5\%}_{-5\%}\right)$	$3.41^{+0.26}_{-0.16}\left(^{+8\%}_{-5\%}\right)$
40-60%	$7.4^{+0.4}_{-0.6}\left(^{+6\%}_{-8\%}\right)$	$6.6^{+0.4}_{-0.4}\left(^{+6\%}_{-6\%}\right)$	$6.31^{+0.5}_{-0.34}\left(^{+8\%}_{-5\%}\right)$
30-40%	$9.8^{+0.6}_{-0.6}\left(^{+6\%}_{-6\%}\right)$	$9.2^{+0.5}_{-0.5}\left(^{+6\%}_{-6\%}\right)$	$8.9^{+0.6}_{-0.5}\left(^{+7\%}_{-5\%}\right)$
20-30%	$11.4^{+0.6}_{-0.6}\left(^{+6\%}_{-6\%}\right)$	$11.2^{+0.6}_{-0.7}\left(^{+6\%}_{-6\%}\right)$	$11.1^{+0.7}_{-0.6}\left(^{+6\%}_{-6\%}\right)$
10-20%	$13.0^{+0.8}_{-0.7}\left(^{+6\%}_{-6\%}\right)$	$13.7^{+0.8}_{-0.8}\left(^{+6\%}_{-7\%}\right)$	$14.1^{+0.9}_{-0.8}\left(^{+6\%}_{-6\%}\right)$
5-10%	$14.6^{+1.2}_{-0.8}\left(^{+8\%}_{-6\%}\right)$	$16.5^{+1.0}_{-1.0}\left(^{+6\%}_{-6\%}\right)$	$17.4^{+1.1}_{-1.1}\left(^{+7\%}_{-6\%}\right)$
1-5%	$16.1^{+1.7}_{-0.9}\left(^{+11\%}_{-6\%}\right)$	$19.5^{+1.3}_{-1.3}\left(^{+7\%}_{-7\%}\right)$	$21.4^{+1.4}_{-2.0}\left(^{+7\%}_{-9\%}\right)$
0-1%	$18.2^{+2.7}_{-1.0}\left(^{+15\%}_{-5\%}\right)$	$24.1^{+1.6}_{-2.0}\left(^{+7\%}_{-8\%}\right)$	$27.4^{+1.6}_{-4}\left(^{+6\%}_{-16\%}\right)$
0-90%	$8.4^{+0.5}_{-0.4}\left(^{+6\%}_{-5\%}\right)$	$8.5^{+0.5}_{-0.5}\left(^{+6\%}_{-5\%}\right)$	$8.6^{+0.5}_{-0.4}\left(^{+6\%}_{-5\%}\right)$

ATLAS Results:
dN/dη p-Pb ATLAS (0-90%) vs ALICE (MinBias)

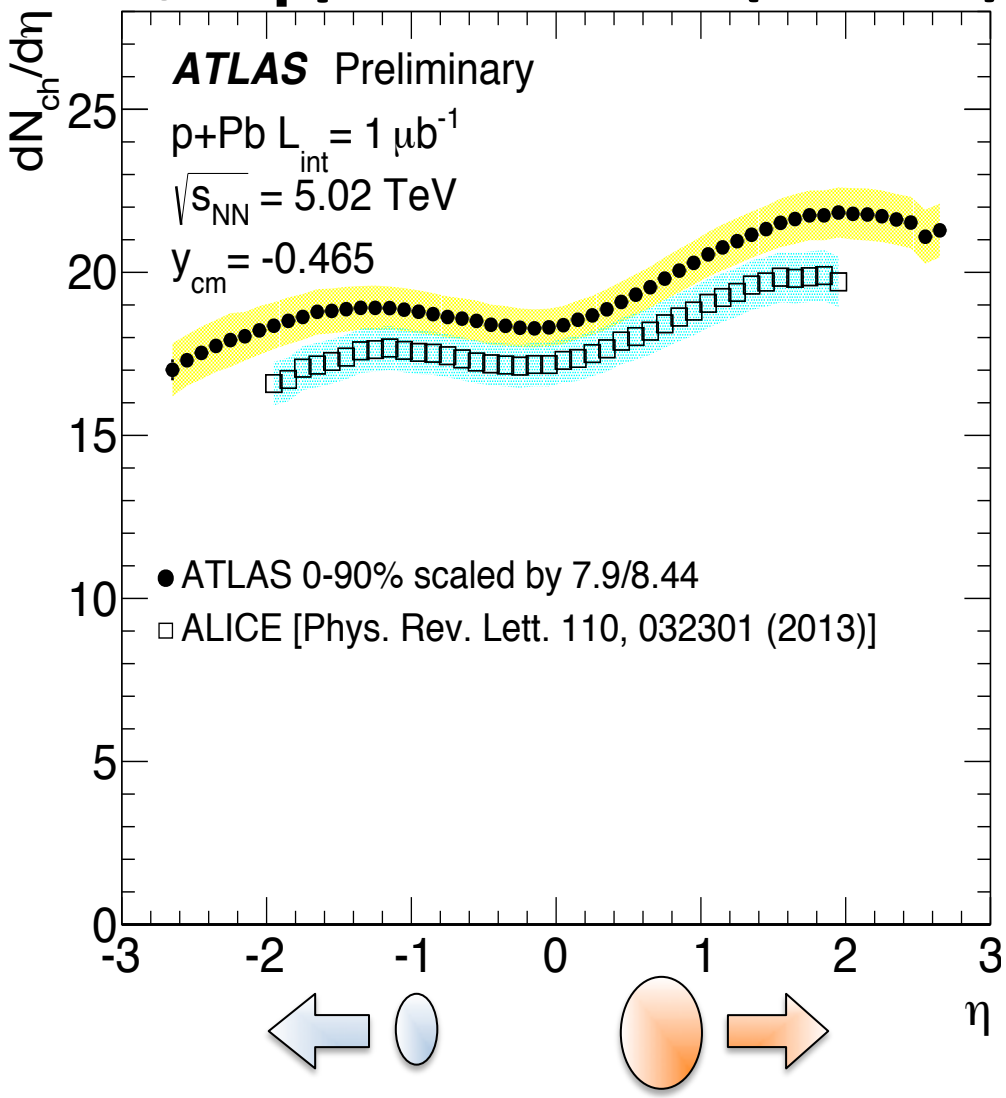

- ALICE MinBias:

0-98% N_{part} = 7.9 (±7.6%)

- ATLAS:

0-90% N_{part} = 8.44 (+5.6%, -4.9%)

- ATLAS points are scaled by the ratio
- ALICE makes no gap cleaning and have a statement of non diffractive events

Motivation to study p-Pb collisions:

- Disentangle initial and final state effects.
- Probe nuclear wave function at small x.
- Investigate QCD at high gluon density: shadowing and gluon saturation.
- Study diffractive and photo-nuclear excitations

Elements of both pp and heavy ion collisions: